Multi-Edge-Type LDPC Code Concatenated with Trellis Shaping for PAR Reduction

Abdul Wakeel and Werner Henkel
Transmission Systems Group (TrSyS)
Jacobs University Bremen
Bremen 28759, Germany
Email: wakeel44@gmail.com and werner.henkel@ieee.org

***Abstract*—This manuscript addresses optimization of irregular Low-Density Parity-Check (LDPC) code concatenated with Trellis Shaping for Peak-to-Average Ratio (PAR) reduction in Orthogonal Frequency Division Multiplexing (OFDM) systems. It takes into account the different error probabilities inside a QAM constellation and from the decoding of the MSBs of the Trellis Shaping.**

***Index Terms*—Irregular LDPC, Trellis Shaping, Peak-to-Average Ratio (PAR)**

I. Introduction

A major drawback of OFDM systems is high PAR, which is defined as

$$\mathrm{PAR}(\mathbf{x}) = \frac{\max_{k,1\leq k\leq N}\ |x_k|^2}{E\{|x_k|^2\}}\ , \qquad (1)$$

where $\max_k |x_k|^2$ represents the amplitude of the maximum peak power of the envelope and $E\{|x_k|^2\}$ denotes the average power over an interval $1 \leq k \leq N$ of the OFDM symbol $\mathbf{x}$. Different techniques have been proposed to limit the peak excursion of an OFDM signal. The well-known techniques amongst them are Clipping, Selected Mapping, Partial Transmit Sequences, and Tone Reservation [1], [2]. An also very promising technique in terms of PAR reduction with a moderate complexity is Trellis-Shaping, orinally introduced by Forney [3] for reducing the average power. A combination of shaping and protograph-based LDPC codes developed in [4] shows procedural similarities independently developed from ours, adapted for power shaping instead of PAR reduction that we focus on. Trellis-Shaping for PAR reduction, we first proposed in [5]. The idea was later extended by Ochiai [6], where the author devised a new branch metric based on the autocorrelation of the side-lobes in the DFT domain. Conventionally, hard decision decoding was used to extract the input bit stream from the shaping code sequence. However, to improve the system performance, the authors in [7] suggested soft decision decoding using the BCJR algorithm based on the compound trellis of the inverse syndrome former $(\mathbf{H}^{-1})^T$ and the shaping code $\mathcal{C}_s$. To enhance the system performance further in terms of BER, the authors concatenated a regular LDPC code with Trellis Shaping for PAR reduction of a BICM-OFDM system. They used higher order $\mathcal{M}$-ary QAM modulation (256-QAM) as modulated symbols at each tone of the OFDM system. However, as it is well known from literature, an irregular LDPC code has a better performance than a regular one. Moreover, in higher order constellations ($\mathcal{M}$-ary QAM), the bits constituting the QAM-symbol have different error probabilities. Thus, there is a possibility to design an irregular LDPC code taking into account the bit-error probabilities of the individual bits inside an $\mathcal{M}$-ary QAM symbol.

The rest of the paper first starts from a representation of the equivalent binary channels of an $\mathcal{M}$-ary QAM modulation in Section II. Section III provides the system model and a brief introduction to Trellis Shaping, particulary to Sign-bit Shaping in Section III-A. Optimization of the variable-node degree distribution and simulation results are presented in sections III-B and IV, respectively.

II. Equivalent binary channels of $\mathcal{M}$-ary QAM

As we know, the bits inside a higher order $\mathcal{M}$-ary QAM constellation have different error probabilities, depending on the size, the type, and the labeling of the constellation used. Let $P_{b_i}, b_i = \{b_1, b_2, \ldots b_B\}$, where $B = \log_2(\mathcal{M})$ and $\mathcal{M}$ is the constellations size, be the error probability of the ith bit. Bits with the same error probabilities, i.e., $P_{b_i} = P_{b_j}$, are assigned to subgroups, which we will subsequently call modulation classes, i.e., $\mathbf{M} = \{M_1, M_2, \ldots, M_{N_m}\}$, where $N_m = B/2$ for a square Gray-coded QAM [8]. The standard deviations for all modulation classes, $\boldsymbol{\sigma} = \{\sigma_1, \sigma_2, \ldots, \sigma_{N_m}\}$, are then calculated from the bit-error probabilities of each modulation class P_{b,M_i} using an equivalent BPSK channel description [9] as shown in Fig. 1, and is defined as

$$\sigma_i^2 = \frac{1}{2\{\mathrm{erfc}(2P_{b,M_i})\}^2}\ , \qquad (2)$$

where $\boldsymbol{\sigma}$ is a vector for the equivalent noise of the individual channels. This irregularity of the individual bits inside a QAM

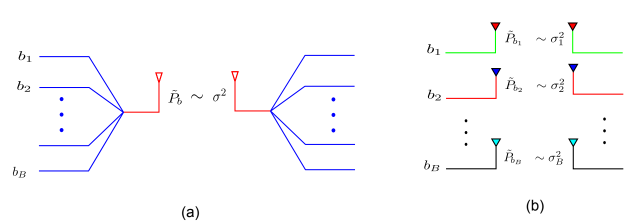

Fig. 1. Binary channel assumption (a) physical channel (b) equivalent binary channels

symbols can be exploited to optimize an LDPC code, as the individual bits have different error probabilities and thus can be protected differently inside the same QAM symbol. Note that we have used a Gaussian model for the individual channels, which will also carry over to the intrinsic LLR computation in the LDPC decoder. If modifications in that individual channels will be required, this will also mean different LLR expressions and actual convolution steps in density evolution.

III. System Model

A basic block diagram of serial concatenation of an irregular LDPC code with Trellis Shaping is shown in Fig. 2. The input bit sequence $\mathbf{u}$ is first encoded using an irregular LDPC code. The encoded bits $\mathbf{c}$ are then passed through a Trellis Shaper, which is used to define the sequence of $\mathcal{M}$-ary QAM symbols $\mathbf{X}$. After serial-to-parallel conversion, $\mathbf{X}$ is transformed into time-domain using the Inverse Discrete Fourier Transform (IDFT) modulator defined as

$$x_k = \frac{1}{\sqrt{N}} \sum_{n=1}^{N} X_n e^{j\frac{2\pi nk}{N}} \qquad , \ 1 \leq k \leq N \ , \tag{3}$$

where x_k is the kth sample of the discrete time sequence $\mathbf{x} = [x_k]$, $k = 1, 2, \ldots, N$, and N is the frame size. After parallel-to-serial conversion and appending a cyclic prefix, the time domain signal is transmitted over a channel. At the receiver, reverse operation are performed to recover the useful information. The Log-Likelihood Ratios (LLRs) obtained are passed into an LDPC decoder to obtain an estimate of the transmit sequence. We will give an insight to each block, subsequently

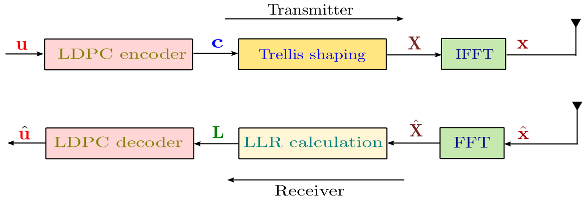

Fig. 2. Irregular LDPC code concatenated with Trellis Shaping

A. Trellis Shaping

We consider sign-bit shaping with a binary convolutional shaping code as has been presented in [3].

A simplified block diagram of a trellis shaper is shown in Fig. 3. In there, $\mathcal{C}_s$ is a binary rate $R = \frac{k}{n} = \frac{1}{2}$ convolutional code (also referred to as the shaping code) with a 1×2 generator matrix $\mathbf{G}$, where k and n stands for the number of input and output bits, respectively. $\mathbf{H}^T$ and $(\mathbf{H}^{-1})^T$ are the 2×1 parity-check matrix (syndrome former) and its 1×2 left inverse (inverse syndrome former), respectively. Let $\mathbf{c}$ be the input data sequence of length $1 \times (B-1) \cdot N$ prior to constellation mapping, which will be transmitted with an OFDM frame of size N. The input bit stream $\mathbf{c}$ is demultiplexed into two sets of sequences $\mathbf{m}$ and $\mathbf{n}$. $\mathbf{m}$ is used

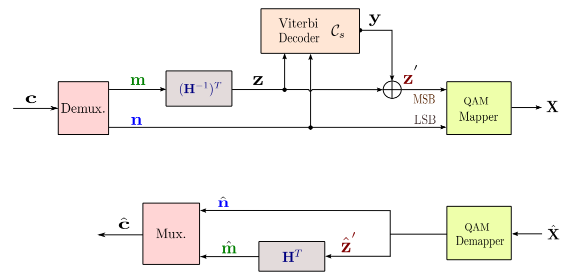

Fig. 3. Block diagram of Trellis Shaping

to choose the MSBs, which are used to select one out of the four quadrants, while $\mathbf{n}$ is for the LSBs which address a particular point inside a quadrant.

In TS, valid codeword in the shaping code $\mathcal{C}_s$ is selected which minimizes the PAR of the transmit signal $\mathbf{x}$, based on a metric in the Viterbi algorithm. Along with the LSBs $\mathbf{n}$, the MSBs $\mathbf{z}^{'}$ determines the nth QAM symbol as

$$X_n = \mathcal{M}(\mathbf{z}_n^{'}; \mathbf{n}_n) = \mathcal{M}(\mathbf{z}_n \oplus \mathbf{y}_n; \mathbf{n}_n) \ . \tag{4}$$

As a metric in the Viterbi algorithm, we consider minimization of the aperiodic autocorrelation function of the side lobes, as proposed by Ochiai in [6], defined as

$$\mu^i = \mu^{i-1} + \sum_{m=1}^{i-2} 2\Re e \left(R_m^{(i-1)*} \delta_m^{i-1} \right) + \sum_{m=1}^{i-1} \left| \delta_m^{i-1} \right|^2 \ , \tag{5}$$

where R_m^i is the aperiodic autocorrelation of the QAM symbols at length i, $\mu^i = \sum_{m=1}^{i} |R_m^i|^2$, and $\delta_m^i = X_i X_{i-m}^*$.

To retrieve the input bit sequence $\mathbf{m}$ correctly, at the transmitter, the input bit sequence $\mathbf{m}$ is preprocessed using the left inverse syndrome former $(\mathbf{H}^{-1})^T$ of the shaping code $\mathcal{C}_s$. At the receiver, the received sequence is postprocessed using the syndrome former $\mathbf{H}^T$ of $\mathcal{C}_s$. For a valid codeword $\mathbf{y}$, $\mathbf{H}\mathbf{y}^T = 0$, $\mathbf{m}$ is then decoded as

$$\mathbf{z}^{'}\mathbf{H}^T = (\mathbf{z} \oplus \mathbf{y})\mathbf{H}^T = \mathbf{z}\mathbf{H}^T \oplus \underbrace{\mathbf{y}\mathbf{H}^T}_{=0} = \mathbf{z}\mathbf{H}^T = \mathbf{m}\underbrace{(\mathbf{H}^{-1})^T\mathbf{H}^T}_{=I}$$

However, instead of using the hard decision decoding described earlier, we will use the soft decision decoding with the BCJR algorithm, based on the compound trellis of the inverse syndrome former and the shaping code as proposed in [7], to obtain the LLRs for the shaping bit sequence.

The LLRs obtained from the BCJR algorithm for the MSBs along with the LLRs for the LSBs are fed into an LDPC decoder to obtain the received intrinsic information for the complete bit sequence $\mathbf{u}$. Subsequently, we will give a brief introduction to the LDPC codes followed by optimization of the variable-node degree distribution.

B. Irregular LDPC codes

We design an irregular LDPC code concatenated with Trellis Shaping (Fig. 4) for a better performance of the system as compared to the regular LDPC code solutions [7]. The input bit stream $\mathbf{u}$ is first encoded using the irregular LDPC code.

The encoded bits are then assigned to different modulation classes based on the error probabilities of the individual bits inside the QAM symbol. We exploit the irregularities inside the QAM symbol and design an irregular LDPC code based on the error probabilities of the individual bits. Subsequently, we optimize the variable-node degree distribution for constructing an irregular LDPC code.

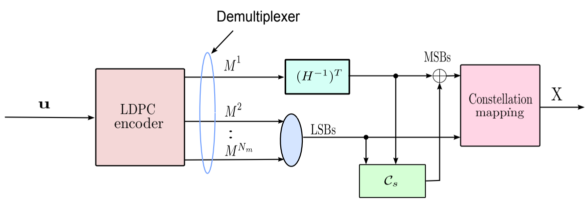

Fig. 4. Block diagram of LDPC code concatenated with Trellis Shaping

1) Notation: Irregular LDPC codes are specified by the variable and check-node degree polynomials

$$\lambda(x) = \sum_{i=2}^{d_{v\,max}} \lambda_i x^{i-1} \qquad \text{and} \qquad \rho(x) = \sum_{i=2}^{d_{c\,max}} \rho_i x^{i-1} \ , \quad (6)$$

where λ_i and ρ_i are the fractions of edges connected to variable and check nodes of degree i, respectively. The rate follows as

$$R = 1 - \frac{\sum_{j=2}^{d_{c\,max}} \rho_j / j}{\sum_{i=2}^{d_{v\,max}} \lambda_i / i} \ . \quad (7)$$

Let the codeword length be N_c. In order to optimize the variable-node degree distribution for the LDPC code, we will make use of the irregularities of the individual bits inside a QAM symbol. Based on the bit-error probabilities of the individual bits constituting a QAM symbol, we define N_m to be the total number of modulation classes. Moreover, let β_i be the proportion of bits in each modulation class given by a vector $\boldsymbol{\beta} = \{\beta_1, \beta_2, \ldots \beta_{N_m}\}$, with, $\beta_j = N_j/N_c$, N_j is the total number of bits in modulation class j and N_c is the codeword length. Let $\boldsymbol{\lambda}$ be the vector of the overall variable node degree distribution for all modulation classes. For a modulation class M_j, $\boldsymbol{\lambda}_{M_j}$ can be written as $\boldsymbol{\lambda}_{M_j} = [\lambda_{M_{j,2}}, \lambda_{M_{j,3}}, \ldots, \lambda_{M_{j,d_{v\,max}}}]^T$, where $\boldsymbol{\lambda}_{M_{j,i}}$ is the sub-degree distribution and represents the proportion of edges connected to a variable node of degree i belonging to the modulation class M_j. The overall variable node degree distribution for the N_m modulation classes is given as

$$\boldsymbol{\lambda} = \left[\boldsymbol{\lambda}_{M_1}, \boldsymbol{\lambda}_{M_2}, \ldots, \boldsymbol{\lambda}_{M_{N_m}}\right]^T \ , \quad (8)$$

where $\{\cdot\}^T$ stands for transpose. Moreover, to construct an irregular LDPC code, we also need the check-node degree distribution. The check-node degree distribution is given by the vector $\boldsymbol{\rho} = [\rho_2, \rho_3, \ldots, \rho_{d_{c\,max}}]^T$.

2) Multi-edge type optimization of the variable-node degree distribution: In order to optimize the variable-node degree distribution for an irregular LDPC code, we will follow the approach of [9], [10]. In the Belief Propagation (BP) algorithm, LLRs are exchanged along the edges between variable and check nodes in an iterative fashion. Let L_{V_i,C_j} be the message from a variable node V_i to a check node C_j. The variable node update rule in BP algorithm is given by

$$L_{V_i,C_j} = L_0 + \sum_{k \neq j} L_{C_k,V_i} \ , \quad (9)$$

where L_0 is the channel output and the summation is over all the neighboring check nodes excluding C_j. Similarly, for check node messages L_{C_j,V_i}, we have

$$L_{C_j,V_i} = 2 \tanh^{-1}\left(\prod_{k \neq i} \tanh(L_{V_k,C_j})\right) \ , \quad (10)$$

where the product is over all variable nodes excluding V_i. At the l^{th} iteration, the mutual information from a check node to the variable node x_{cv} and from a variable node to a check node x_{vc} computed for a standard LDPC code using density evolution (DE) with Gaussian approximation, [9], [10], can be expressed as

$$x_{cv}^{(l-1)} = 1 - \sum_{j=2}^{d_{c\,max}} \rho_j J\left(\sqrt{(j-1)J^{-1}(1 - x_{vc}^{(l-1)})}\right) \ , \quad (11)$$

$$x_{vc}^{(l)} = \sum_{i=2}^{d_{v\,max}} \lambda_i J\left(\frac{2}{\sigma^2} + (i-1)J^{-1}(x_{cv}^{(l-1)})\right) \ , \quad (12)$$

where $J(.)$ computes the mutual information, i.e., $x = J(m)$ given as

$$J(m) = 1 - \frac{1}{\sqrt{4\pi m}} \int_{\mathbb{R}} \log_2(1 + e^{-z}) \cdot e^{-\frac{(z-m)^2}{4m}} dz \ , \quad (13)$$

where $z \sim N(m, 2m)$ is a consistent Gaussian random variable. In our analysis, the variable node degree distribution is split into sub-groups based on the modulation classes N_m. Thus, we adapt and modify Eq. (12) as

$$x_{vc}^{(l)} = \sum_{j=1}^{N_m} \sum_{i=2}^{d_{v\,max}} \lambda_{M_{j,i}} J\left(\frac{2}{\sigma_j^2} + (i-1)J^{-1}(x_{cv}^{(l-1)})\right) \ . \quad (14)$$

With equations (11) and (14), the density evolution for the mutual information of the LDPC code, with N_m sub-class variable-node degrees is summarized as

$$x_{vc}^{(l)} = F(\boldsymbol{\lambda}, \boldsymbol{\rho}, \boldsymbol{\sigma}^2, x_{vc}^{(l-1)}) \ . \quad (15)$$

We need to ensure the mutual information to increase per iteration, i.e.,

$$F(\boldsymbol{\lambda}, \boldsymbol{\rho}, \boldsymbol{\sigma}^2, x_{vc}^{(l-1)}) \ > \ x_{vc}^{(l-1)} \ . \quad (16)$$

Another important constraint to be fulfilled by the ensemble LDPC code is the stability constraint which ensures convergence of the mutual information close to one. The stability condition gives an upper limit for degree-2 variable nodes [10],

$$\frac{1}{\lambda'(0)\rho'(1)} > e^{-r} = \int_{\mathbb{R}} P_0(x) e^{-\frac{x}{2}} dx = e^{-\frac{1}{2\sigma^2}} \ , \quad (17)$$

with $P_0(x)$ being the message density for the received values and $\lambda'(x)$ and $\rho'(x)$ being the derivatives of the degree polynomials. The bits in our schemes experience different channel noise with different equivalent noise variances σ_j^2, thus, we exploit the average density, given by utilizing the modulation class proportions β,

$$e^{-r} = \int_{\mathbb{R}} \sum_{j=1}^{N_m} \beta_j \cdot P_{0,j}(x) e^{-\frac{x}{2}} dx = \sum_{j=1}^{N_m} \beta_j \cdot e^{-\frac{1}{2\sigma_j^2}} \; . \quad (18)$$

Splitting the variable-node degree distribution into subclasses results in a sum constraint. For the algorithm to converge, the sum constraint is formulated as [9]

$$\sum_{j=1}^{N_m} \sum_{i=2}^{d_{v_{max}}} \lambda_{M_{j,i}} = 1 \; . \quad (19)$$

3) Optimization algorithm: With all the constraints and characterization for the density evolution algorithm, we optimized the variable-node degree distribution with a maximum degree $d_{v_{max}}$. Our strategy was to optimize the variable-node degree distribution which maximizes the code rate. We modified the optimization algorithm proposed in [9], [11]. The linear programming routine requires the check-node degree distribution $\boldsymbol{\rho}$, the maximum variable node degree $d_{v_{max}}$, proportion of the bits in various modulation classes $\boldsymbol{\beta}$, the required code rate R and the variance vector $\boldsymbol{\sigma}^2$ derived from the bit-error probabilities of different modulation classes. After obtaining an optimized variable-node degree distribution, the parity-check matrix $\mathbf{H}$ is constructed using the Progressive-Edge-Growth (PEG) algorithm.

IV. Results and discussion

For the simulation results, we have considered an OFDM system with 128 sub-carriers, square 256-QAM, and Gray labeling (Type-I in [6]). We use a rate-6/7 LDPC codes (both regular and irregular codes) each of length $N_c = 896$, in order to match one OFDM frame. The LDPC code is concatenated with Trellis Shaping which adds 1 bit of redundancy per QAM symbol, thus the overall code-rate then equals 3/4. In order to decode the LDPC codeword, we use BP with 50 iterations. We also compare our results to a system without Trellis Shaping. The codeword length and the code rate for such codes are chosen to be 1024 and 3/4, respectively.

As shown in the Fig. 2, the input bit stream $\mathbf{u}$ is first encoded with an optimized irregular LDPC code. In order to optimize the LDPC code, we exploit the bit-error probabilities of the individual bits inside the M-ary QAM symbol. For the 256-QAM constellation with Gray mapping $B = 8$, i.e., each QAM symbol maps 8 bits, thus, we have $N_m = 4$ modulation classes. The bit-error probabilities of these modulation classes are given as $\mathbf{P}_{b,i} = \{P_{b,M_1}, P_{b,M_2}, P_{b,M_3}, P_{b,M_4}\}$. Out of the 8 bits, the first 2 bits with error probability P_{b,M_1} are used to select the MSBs while the last 6 bits are used to choose the LSBs. For the 256-QAM constellation, we will use the exact bit-error probability formulas as derived in [8][1] to compute the individual noise standard deviations for the different modulation classes, $\boldsymbol{\sigma} = \{\sigma_1, \sigma_2, \sigma_3, \sigma_4\}$ using Eq. (2).

For the LSBs with bit-error probabilities $\{P_{b,M_2}, P_{b,M_3}, P_{b,M_4}\}$, no preprocessing is performed, thus, the noise variance of the individual modulation classes is obtained directly using Eq. (2). However, for the MSBs, which are preprocessed by the inverse syndrome former $(\mathbf{H}^{-1})^T$, in order to calculate the standard deviation σ_1, we must take the bit-error probability of the $(\mathbf{H}^{-1})^T$ $P_{b_{sf}}$ into consideration along with P_{b,M_1} as well. From the P_{b,M_1} of the first modulation class of the 256-QAM constellation, we can easily calculate the standard deviation σ_{M_1} using Eq. (2). Next, we try to compute the bit-error probability for the $(\mathbf{H}^{-1})^T$. For trellis shaping, we considered the (5,7) shaping code $\mathcal{C}_s$, with a generator matrix $\mathbf{G}$, defined as $(1 + D^2, 1 + D + D^2)$. We choose (2,3), i.e., $(D, 1 + D)$ as a left inverse of the syndrome former $(\mathbf{H}^{-1})^T$ of the shaping code $\mathcal{C}_s$ [3]. Based on the weight distribution of the code, the bit-error probability of the input bits encoded by the $(\mathbf{H}^{-1})^T$ can be calculated by exploiting the Union bound. Restricting it to the first term at d_{free}, the Chernoff bound yieds

$$P(b) \approx \frac{1}{k}\frac{1}{2} B_{d_{free}} \left(e^{-\frac{E_s}{N_0}}\right)^{d_{free}} \; , \quad (20)$$

where $B_{d_{free}}$ represents the total number of erroneous bits at a distance d_{free}. Sign-bit shaping with rate-$1/2$ means an inverse syndrome former with $k = 1$. Moreover, from the transfer function, $B_{d_{free}} = 1$, and $d_{free} = 3$ for $(\mathbf{H}^{-1})^T$.[2]

Now, the input bit sequence encoded by the inverse syndrome former sees a channel with a standard deviation defined by σ_{M_1}. With these values, the final bit-error probability $P_{b_{sf}}$ for the input bit sequence encoded by the inverse syndrome former is formulated as

$$P_{b_{sf}} \approx \frac{1}{2} \left(e^{-\frac{S}{N}}\right)^3 \; , \quad (21)$$

where $S/N = E_s/N_0$ with $N = \sigma_{M_1}^2$. Using Eq. (2), the noise variance σ_1^2 for the MSBs, can be calculated as

$$\sigma_1^2 = \frac{1}{2\{\mathrm{erfc}(2P_{b_{sf}})\}^2} \; . \quad (22)$$

The vector of standard deviations $\boldsymbol{\sigma}$ for the individual modulation classes is then given as $\boldsymbol{\sigma} = [\sigma_1, \sigma_2, \sigma_3, \sigma_4]$. σ_i is the standard deviation of the ith modulation class of the 256-QAM constellation.

Based on $\boldsymbol{\sigma}$, we optimize the variable-node degree distribution $\boldsymbol{\lambda}$ for a given check-node degree distribution $\boldsymbol{\rho}$. The check-node degree distribution $\rho(x)$ considered herein is $\rho(x) = 0.8266\ x^{34} + 0.1345\ x^{35} + 0.0087\ x^{70} + 0.0302\ x^{71}$ [10]. Other parameters required for the optimization of the degree distribution are, $R = 6/7$, $d_{v_{max}} = 30$ and the proportion of bits in each modulation class $\boldsymbol{\beta} = [128/896, 256/896, 256/896, 256/896]$. Table I shows the optimized variable-node degree distribution using the procedure

[1] The authors in [8] gives the expression for a noise with $N_0/2$ power spectral density, however, we have modified the expressions for a noise with N_0 power spectral density, i.e., we use a two-sided definition.

[2] For (D, 1+D) inverse syndrome former $(\mathbf{H}^{-1})^T$, the transfer function is given as $\mathcal{T}(D) = \frac{D^3}{1+D} = D^3 + D^4 + \ldots$

TABLE I

VARIABLE-NODE DEGREE DISTRIBUTIONS FOR IRREGULAR LDPC WITH/WITHOUT CONCATENATED WITH TRELLIS SHAPING, FOR A 256-QAM CONSTELLATION WITH GRAY MAPPING, $N_m = 4$ MODULATION CLASSES.

	with TS	without TS
M_1	$\lambda_3 = 0.08583$	$\lambda_6 = 0.03682$ $\lambda_7 = 0.02237$ $\lambda_{30} = 0.58173$
M_2	$\lambda_3 = 0.0243$ $\lambda_6 = 0.29473$	$\lambda_{12} = 0.17234$
M_3	$\lambda_2 = 0.05175$ $\lambda_6 = 0.10605$ $\lambda_7 = 0.09568$	$\lambda_2 = 0.04595$ $\lambda_6 = 0.03446$
M_4	$\lambda_2 = 0.08975$ $\lambda_7 = 0.03603$ $\lambda_{30} = 0.21588$	$\lambda_2 = 0.04207$ $\lambda_6 = 0.04159$ $\lambda_{30} = 0.02266$

as sketched in Section III-B2 and Section III-B3. Table I also shows the variable-node degree distribution for an irregular LDPC code without trellis shaping, with parameters, $R = 3/4$, $N_c = 1024$, $d_{v_{max}} = 30$, and $\boldsymbol{\beta} = [0.25, 0.25, 0.25, 0.25]$.

After obtaining the optimized variable node degree distribution, we next constructed the $\mathbf{H}$ matrix using the PEG algorithm.

A. Performance at the transmitter, PAR reduction

Figure 5 shows the CCDF of the PAR for an OFDM system with and without Trellis Shaping. A gain of approximately 4.1 dB at 10^{-5} can be obtained using Trellis Shaping.

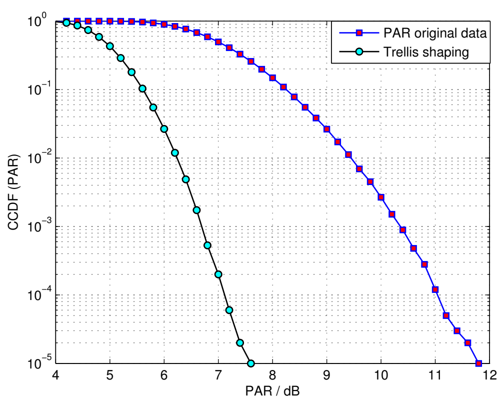

Fig. 5. CCDF(PAR) of Trellis Shaping for OFDM system, N = 128

B. FER of irregular vs. regular LDPC codes

For performance comparison, we consider a (3,21) regular LDPC code with the same specs as the irregular LDPC code. For the $\mathbf{H}$ matrix of the regular LDPC code we used the random construction.

Figure 6 shows the performance curves for irregular and regular LDPC codes. In case of Trellis Shaping, the system performance can be improved by 0.6 dB when using irregular LDPC codes as compared to regular LDPC codes. The figure also shows the FER curves for a system using LDPC codes concatenated with OFDM without Trellis Shaping. Even for the systems without Trellis Shaping the irregular LDPC codes outperforms the regular codes. Despite of having incorporated the rate loss by using E_b/N_0, the gap between curves of the LDPC code concatenated with Trellis Shaping and without Trellis Shaping is primarily due to the different code rates used, i.e., 6/7 in case of Trellis Shaping and 3/4 without Trellis Shaping.

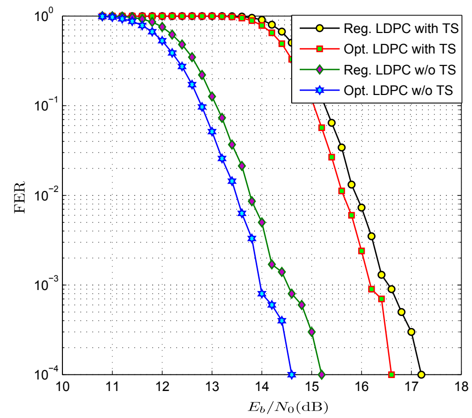

Fig. 6. FER curves for irregular vs. regular LDPC codes with and without Trellis Shaping

V. SUMMARY

For the irregular LDPC code, we optimized the variable-node degree distribution based on the irregularities of the individual bits inside a higher order $\mathcal{M}$-ary QAM constellation. For the input bit sequence encoded by the inverse syndrome former, the bit-error probability was computed based on the transfer function of the inverse syndrome former. The LLRs for the shaping code sequence were obtained using a BCJR algorithm based on the compound trellis of the shaping code and the inverse syndrome former. The system performance can be improved by concatenating an irregular LDPC code with Trellis Shaping.

REFERENCES

[1] J. Tellado, *Peak-to-average power reduction for multicarrier modulation*, Ph.D. thesis, Stanford University, 1999.

[2] W. Henkel and V. Zrno, "PAR reduction revisited: an extension to Tellado's method," *6th Intern. OFDM Workshop*, Hamburg, Germany, Sept. 2001.

[3] G. D. Forney, "Trellis Shaping," *IEEE Tr. on Inf. Theory*, Vol. 38, pp. 281-300, March 1992.

[4] F. Steiner, G. Böcherer, and G. Liva, "Protograph-Based LDPC Code Design for Shaped Bit-Metric Decoding," *IEEE JSAC*, Vol. 34, No. 2, pp. 397-407, Feb. 2016.

[5] W. Henkel and B. Wagner, "Another application for Trellis Shaping: PAR reduction for DMT (OFDM)," *IEEE Tr. on Comm.*, Vol. 48, No. 9, pp. 1471-1476, Sept. 2000.

[6] H. Ochiai, "A novel Trellis-Shaping design with both peak and average power reduction for OFDM systems," *IEEE Tr. on Comm.*, Vol. 52, No. 11 pp. 1916-1926, Nov. 2004.

[7] R. Yoshizawa and H. Ochiai, "A serial concatenation of coding and trellis shaping for OFDM systems with peak power reduction," *IEEE ISIT* , Cambridge, USA, July 2012.

[8] D. Yoon, K. Cho, and J. Lee, "Bit error probability of $\mathcal{M}$-ary quadrature amplitude modulation," *VTC*, Massachusetts, USA, Sept. 2000.

[9] S. Sandberg and N. von Deetzen, "Design of bandwidth efficient unequal error protection LDPC codes," *IEEE Trans. on Comm.*. Vol. 58, No. 3, pp. 802-811, March 2010.

[10] T. J. Richardson, M. A. Shokrollahi, and R. L. Urbanke, "Design of capacity-approaching irregular low-density parity-check codes," *IEEE Trans. on Inf. Th.*, Vol. 47, No. 2, pp. 619-637, Feb. 2001.

[11] A. Filip and W. Henkel, "Hierarchical modulation to support low-density parity-check code design?," *9th International ITG Conf. on Source and Channel Coding*, Munich, Germany, Jan. 2013.